J|A|C|S
ARTICLES

Published on Web 11/26/2008

The Amyloid-β Peptide of Alzheimer's Disease Binds Cu^{I} in a Linear Bis-His Coordination Environment: Insight into a Possible Neuroprotective Mechanism for the Amyloid-β Peptide

Jason Shearer*,† and Veronika A. Szalai*,‡

Department of Chemistry/216, University of Nevada—Reno, 1664 North Virginia Street, Reno, Nevada 89557, and Department of Chemistry & Biochemistry, University of Maryland Baltimore County, 1000 Hilltop Circle, Baltimore, Maryland 21250

Received July 29, 2008; E-mail: shearer@unr.edu; vszalai@umbc.edu

Abstract: Oxidative stress has been suggested to contribute to neuronal apoptosis associated with Alzheimer's disease (AD). Copper may participate in oxidative stress through redox-cycling between its +2 and +1 oxidation states to generate reactive oxygen species (ROS). In vitro, copper binds to the amyloid-β peptide of AD, and *in vivo*, copper is associated with amyloid plaques characteristic of AD. As a result, the AβCu^{I} complex may be a critical reactant involved in ROS associated with AD etiology. To characterize the AβCu^{I} complex, we have pursued X-ray absorption (XAS) and electron paramagnetic resonance (EPR) spectroscopy of AβCu^{II} and AβCu^{I} (produced by ascorbate reduction of AβCu^{II}). The AβCu^{II} complex Cu K-edge XAS spectrum is indicative of a square-planar Cu^{II} center with mixed N/O ligation. Multiple scattering analysis of the extended X-ray absorption fine structure (EXAFS) data for AβCu^{II} indicates that two of the ligands are imidazole groups of histidine ligands, indicating a $(N_{Im})_2(N/O)_2$ Cu^{II} ligation sphere for AβCu^{II}. After reduction of the AβCu^{II} complex with ascorbate, the edge region decreases in energy by $\sim$4 eV. The X-ray absorption near-edge spectrum region of AβCu^{I} displays an intense pre-edge feature at 8984.1(2) eV. EXAFS data fitting yielded a two-coordinate geometry, with two imidazole ligands coordinated to Cu^{I} at 1.877(2) Å in a linear geometry. Ascorbate reduction of AβCu^{II} under inert atmosphere and subsequent air oxidation of AβCu^{I} to regenerate AβCu^{II} was monitored by low-temperature EPR spectroscopy. Slow reappearance of the AβCu^{II} EPR signal indicates that O_2 oxidation of the AβCu^{I} complex is kinetically sluggish and Aβ damage is occurring following reoxidation of AβCu^{I} by O_2. Together, these results lead us to hypothesize that Cu^{I} is ligated by His13 and His14 in a linear coordination environment in Aβ, that Aβ may be playing a neuroprotective role, and that metal-mediated oxidative damage of Aβ occurs over multiple redox cycles.

Introduction

Alzheimer's disease (AD) is a fatal neurodegenerative disorder that plagues approximately 26 million people worldwide.[1] AD is characterized by a progressive cognitive decline that has been attributed to the deposition of extracellular protein plaques containing the amyloid-β (Aβ) peptide. A single determinant for AD etiology has not been established,[2,3] but oxidative stress induced by reactive oxygen species (ROS) has been hypothesized to be a principal contributor.[4] The redox-active metal ions iron and copper are found in AD plaques,[5] suggesting that they might mediate ROS generation.[6] Thus, answers to fundamental questions regarding the coordination environment and reactivity of these metal ions when bound to Aβ are essential to evaluating their potential role in AD etiology.

The majority of previous studies performed on copper−Aβ adducts were aimed at elucidating the coordination environment

† University of Nevada—Reno.
‡ University of Maryland Baltimore County.

(1) Ferri, C. P.; Prince, M.; Brayne, C.; Brodaty, H.; Fratiglioni, L.; Ganguli, M.; Hall, K.; Hasegawa, K.; Hendrie, H.; Huang, Y.; Jorm, A.; Mathers, C.; Menezes, P. R.; Rimmer, E.; Scazufca, M. *Lancet* **2005**, *366*, 2112.
(2) Castellani, R. J.; Lee, H. G.; Zhu, X.; Perry, G.; Smith, M. A. *J. Neuropathol. Exp. Neurol.* **2008**, *67*, 523. Sergeant, N.; Bretteville, A.; Hamdane, M.; Caillet-Boudin, M. L.; Grognet, P.; Bombois, S.; Blum, D.; Delacourte, A.; Pasquier, F.; Vanmechelen, E.; Schraen-Maschke, S.; Buee, L. *Expert Rev. Proteomics* **2008**, *5*, 207. Cechetto, D. F.; Hachinski, V.; Whitehead, S. N. *Expert Rev. Neurother.* **2008**, *8*, 743. Xia, W. *Curr. Alzheimer Res.* **2008**, *5*, 172. Windisch, M.; Wolf, H.; Hutter-Paier, B.; Wronski, R. *Neurodegener. Dis.* **2008**, *5*, 218. Luheshi, L. M.; Crowther, D. C.; Dobson, C. M *Curr. Opin. Chem. Biol.* **2008**, *12*, 25. Shi, Q.; Gibson, G. E. *Alzheimer Dis. Assoc. Disord.* **2007**, *21*, 276. Skovronsky, D. M.; Lee, V. M.; Trojanowski, J. Q. *Annu. Rev. Pathol.* **2006**, *1*, 151. Irvine, G. B.; El-Agnaf, O. M.; Shankar, G. M.; Walsh, D. M. *Mol. Med.* **2008**, *14*, 451. Selkoe, D. J. *Behav. Brain Res.* **2008**, *192*, 106.
(3) Green, K. N.; Smith, I. F.; Laferla, F. M. *Subcell. Biochem.* **2007**, *45*, 507.
(4) Zhu, X.; Su, B.; Wang, X.; Smith, M. A.; Perry, G. *Cell. Mol. Life Sci.* **2007**, *64*, 2202.
(5) Dong, J.; Atwood, C. G.; Anderson, V. E.; Siedlak, S. L.; Smith, M. A.; Perry, G.; Carey, P. R. *Biochemistry* **2003**, *42*, 2768. Beauchemin, D.; Kisilevsky, R. *Anal. Chem.* **1998**, *70*, 1026. Miller, L. M.; Wang, Q.; Telivala, T. P.; Smith, R. J.; Lanzirotti, A.; Miklossy, J. *J. Struct. Biol.* **2006**, *155*, 30.
(6) Adlard, P. A.; Bush, A. I.; Adman, E. T. *J. Alzheimer's Dis.* **2006**, *10*, 145.

 10.1021/ja805940m CCC: $40.75

of Cu^{II} bound to the peptide.[6−11] Although some work has focused on the ROS reactions catalyzed by the AβCu complex,[10,12,13] information regarding the structure and reactivity of the AβCu^{I} complex is scarce.[14−16] Previous extended X-ray absorption fine structure (EXAFS) measurements of AβCu^{II} led to a model in which the Cu^{II} ion binds to Aβ in a five-coordinate square-pyramidal ligand environment created by coordination to three His imidazoles, an oxygen atom donor (Tyr), and an axial water molecule. Results from other X-ray absorption spectroscopy (XAS) measurements proposed a six-coordinate Cu^{II} species bound to three His imidazoles, Glu/Asp residues, and a water molecule.[17] These structural models are inconsistent with four-coordinate Cu^{II} in the Cu^{II}−Aβ adduct, a geometry that has been suggested on the basis of other spectroscopic data and recent theoretical work.[8,9,18,19]

Recent X-ray absorption near-edge spectroscopy (XANES) data indicated that the AβCu^{II} complex can be reduced by ascorbate and 6-hydroxydopamine, but not by cholesterol or dopamine.[15] In another study, Maiti et al. reduced the AβCu^{II} complex with sodium borohydride, a nonphysiological reductant, and followed the reduction reaction with electron paramagnetic resonance (EPR) and fluorescence spectroscopies.[14] Ascorbate radical and hydroxyl radical (either via fluorescence detection or spin-trapped adducts) have been detected upon redox-cycling of the AβCu system.[13,20] In none of these works was the AβCu^{I} complex generated under an inert atmosphere, nor was the O_2 reactivity of the AβCu^{I} complex probed over time.[14] Furthermore, quantification of the amount of AβCu^{II} produced following air oxidation was never rigorously assessed.

Herein we present XAS data of both the AβCu^{II} and AβCu^{I} complexes along with EPR spectroscopic monitoring of the reduction and reoxidation of the AβCu complex. These studies will demonstrate that the Cu^{I} ion forms a stable, well-defined adduct with Aβ. Furthermore, oxidation of Cu^{I} to Cu^{II} by O_2 is kinetically sluggish yet nonetheless affords Aβ damage. The biological implications of these new findings and their implications for AD will be discussed.

Materials and Methods

Materials. Aβ40 and Aβ16 peptides were purchased from Bachem (King of Prussia, PA) or rPeptide (Athens, GA) or synthesized on a Protein Technologies PS3 peptide synthesizer using standard Fmoc chemistries and subsequently purified by high-performance liquid chromatography (HPLC) as previously described.[11] The amino acid sequence for the Aβ40 peptide is DAEFRHDSGYEVHHQKLVFFAEDVGSNKGAIIGLMVGGVV; the amino acid sequence of Aβ16 is the first 16 amino acids of Aβ40. Biological grade glycerol, sodium phosphate, 1,1,1,3,3,3-hexafluoroisopropanol (HFIP), and sodium chloride were purchased from Fisher Scientific (Pittsburgh, PA). Bovine serum albumin (BSA) standards were purchased from Sigma-Aldrich (St. Louis, MO). Quartz EPR tubes were purchased from Wilmad (Buena, NJ). Solutions were prepared in MilliQ water (resistivity >18 mΩ, total organic content <35 ppb). Sodium ascorbate was purchased from Spectrum Chemicals (Gardena, CA). Na_2IrCl_6 was from Alfa-Aesar (Ward Hill, MA).

Sample Preparation. Aβ peptides were monomerized with HFIP and stored at −80 °C in HFIP as previously reported.[18,21] Peptide stock solution in HFIP was removed via a Hamilton gastight syringe that had been washed previously with multiple volumes of HFIP. An aliquot of the peptide stock in HFIP was removed for peptide concentration determination using a BSA calibration curve.[18,21] Immediately prior to making peptide samples, HFIP was removed using a spin-vacuum system. This protocol produces homogeneous solutions of monomeric peptide.[22]

Samples of soluble Aβ16 or Aβ40 were prepared by resuspending dried peptide into buffer containing 50 mM NaP_i, 75 mM NaCl, pH 7.2, with 50% glycerol (v/v). The Aβ16 peptide was used to model Cu(II) binding to soluble Aβ because it is well-established that this region contains the high-affinity Aβ Cu-binding domain[8,9,18,23] and because it does not contain the fibrillization domain (residues 17−21).[23]

Cu^{II} stock solutions were generated as previously reported.[18,21,24] The Cu^{II} concentration in each EPR sample was determined on the basis of a calibration curve generated from Cu^{II}−imidazole standards in *N*-ethylmorpholine buffer at pH 7.22, containing 50% glycerol (v/v). The concentration of Cu^{II} in each of the EPR standards was assayed by chelation with bathocuproine disulfonic acid (BC) and reduction with ascorbate.[25] The quantity of total copper as $[Cu(BC)_2]^{3-}$ was quantified at 483 nm (ϵ_{483} = 12 500 M^{-1} cm^{-1}).[25] The 0, 25, 50, and 100 μM Cu^{II} standards contained 2.0 ± 1.0, 21 ± 1.0, 61 ± 0.4, and 119 ± 1.2 μM Cu^{II}, respectively.

Assessment of Aβ16 Damage following Multiple Redox Cycles by HPLC. A 1.0 mL, 0.10 mM solution of A$\beta 16Cu^{II}$ was prepared as outlined above using a 1:1 Cu^{II}:Aβ16 stochiometry. Throughout the experiment, aliquots were sampled from the main reaction vessel and analyzed by HPLC on a Waters DeltaPrep 60 equipped with an X-Terra C-18 reverse-phase column (5 μm; 4.6 × 100 mm) using a gradient of 10−45% MeCN (0.1% trifluoroacetic acid) in H_2O (0.1% trifluoroacetic acid) over 25 min. Following the initial analysis of the A$\beta 16Cu^{II}$ solution, the sample was reduced with 1.0 equiv of ascorbate. After 19 h, the sample was reanalyzed by HPLC, rereduced with 1.0 equiv of ascorbate, and then reanalyzed after 19 h. The sample was then rereduced with an additional 1.0 equiv of ascorbate and analyzed a final time after an additional 19 h. In each case, 50 μL of sample was added

(7) Karr, J. W.; Szalai, V. A. *Biochemistry* **2008**, *47*, 5006. Kowalik-Jankowska, T.; Dolejsz-Ruta, M.; Wisniewska, K.; Lankiewicz, L. *J. Inorg. Biochem.* **2001**, *86*, 535. Ma, Q. F.; Hu, J.; Wu, W. H.; Liu, H. D.; Du, J. T.; Fu, Y.; Wu, Y. W.; Lei, P.; Zhao, Y. F.; Li, Y. M. *Biopolymers* **2006**, *83*, 20. Danielsson, J.; Pierattelli, R.; Banci, L.; Graslund, A. *FEBS J.* **2007**, *274*, 46. Lim, K. H.; Kim, Y. K.; Chang, Y.-T. *Biochemistry* **2007**, *46*, 13523. Hou, L.; Zagorski, M. G. *J. Am. Chem. Soc.* **2006**, *128*, 9260.
(8) Syme, C. D.; Nadal, R. C.; Rigby, S. E. J.; Viles, J. H. *J. Biol. Chem.* **2004**, *279*, 18169.
(9) Kowalik-Jankowska, T.; Ruta, M.; Wisniewska, K.; Lankiewicz, L. *J. Inorg. Biochem.* **2003**, *95*, 270.
(10) Jiang, D.; Men, L.; Wang, J.; Zhang, Y.; Chickenyen, S.; Wang, Y.; Zhou, F. *Biochemistry* **2007**, *46*, 9270.
(11) Guilloreau, L.; Damian, L.; Coppel, Y.; Mazarguil, H.; Winterhalter, M.; Faller, P. *J. Biol. Inorg. Chem.* **2006**, *11*, 1024.
(12) Kowalik-Jankowska, T.; Ruta, M.; Wisniewska, K.; Lankiewicz, L.; Dyba, M. *J. Inorg. Biochem.* **2004**, *98*, 940.
(13) Guilloreau, L.; Combalbert, S.; Sournia-Saquet, A.; Mazarguil, H.; Faller, P. *Chembiochem* **2007**, *8*, 1317.
(14) Maiti, N. C.; Jiang, D.; Wain, A. J.; Patel, S.; Dinh, K. L.; Zhou, F. *J. Phys. Chem. B* **2008**, *112*, 8406.
(15) Streltsov, V. A.; Varghese, J. N. *Chem. Commun.* **2008**, *27*, 3169.
(16) Raffa, D. F.; Rickard, G. A.; Rauk, A. *J. Biol. Inorg. Chem.* **2007**, *12*, 147.
(17) Streltsov, V. A.; Titmuss, S. J.; Epa, V. C.; Barnham, K. J.; Masters, C. L.; Varghese, J. N. *Biophys. J.* **2008**, *95*, 3447.
(18) Karr, J. W.; Akintoye, H.; Kaupp, L. J.; Szalai, V. A. *Biochemistry* **2005**, *44*, 5478.
(19) Mantri, Y.; Fioroni, M.; Baik, M. H. *J. Biol. Inorg. Chem.* **2008**, *8*, 1197.
(20) Nakamura, M.; Shishido, N.; Nunomura, A.; Smith, M. A.; Perry, G.; Hayashi, Y.; Nakayama, K.; Hayashi, T. *Biochemistry* **2007**, *46*, 12737.
(21) Karr, J. W.; Kaupp, L. J.; Szalai, V. A. *J. Am. Chem. Soc.* **2004**, *126*, 13534.
(22) Stine, W. B., Jr.; Dahlgren, K. N.; Krafft, G. A.; LaDu, M. J. *J. Biol. Chem.* **2003**, *278*, 11612.
(23) Miura, T.; Suzuki, K.; Kohata, N.; Takeuchi, H. *Biochemistry* **2000**, *39*, 7024.
(24) Karr, J. W.; Szalai, V. A. *J. Am. Chem. Soc.* **2007**.
(25) Moffett, J.; Zika, R. G.; Petasne, R. G. *Anal. Chim. Acta* **1985**, *175*, 171.

to 50 μL of a stock solution containing a 0.10 mM concentration of the peptide H_2N-GAATDAQ-COOH as an internal standard and then analyzed by HPLC. Samples were not stirred throughout the course of the experiment but were agitated by wrist for ~15 s upon addition of ascorbate. The samples remained exposed to air throughout the experiment. All chromatograms were quantified using the software program PeakFit (SeaSolve Software, Inc., Framingham, MA). The chromatograms displayed are baseline-corrected.

EPR Spectroscopy. EPR spectra were collected on a Bruker EMX 6/1 spectrometer equipped with a microwave frequency meter and an Oxford Instruments ESR900 liquid He cryostat system. All spectra were collected with the following experimental parameters: microwave frequency, 9.38 GHz; microwave power, 0.5 mW; modulation amplitude, 10 G; time constant, 40.96 ms; conversion time, 40.96 ms; gain, 5×10^4; eight scans; temperature, 20 K. Spectra of calibration standards were collected every run, and a calibration curve to determine the Cu^{II} concentration was generated. The error associated with Cu^{II} concentrations determined using the calibration curve is estimated to be a maximum of 5−10 μM (about 10%) on the basis of comparison of spectra of the calibration standards collected on different days.

EPR samples for experiments with ascorbate were prepared in quartz EPR tubes capped with a tip-off manifold from Wilmad. Samples were degassed under inert atmosphere (dinitrogen or argon) using three freeze−pump−thaw cycles on a vacuum line. Stock solutions of sodium ascorbate for EPR experiments were prepared by adding solid sodium ascorbate to MilliQ water that had been thoroughly degassed on the vacuum line prior to addition of the solid. Aliquots of sodium ascorbate were removed from the stock solution under a blanket of inert gas and injected into the EPR sample, which was maintained under an inert atmosphere during the process. The addition and mixing was complete in less than 2 min typically.

Air was introduced into the EPR samples by freezing them to 77 K, evacuating the sample headspace on the vacuum line, and admitting air into the headspace. Subsequently, the sample was thawed and mixed by inversion of the tube and its contents several times.

XAS Data Measurement and Analysis. The copper-containing peptide solutions were injected into aluminum sample holders between two windows made of Kapton tape (catalog no. 1205, 3M, Minneapolis, MN) and quickly frozen in liquid nitrogen. The Aβ40Cu^{II} sample was prepared and handled at 0 °C to maintain the monomeric peptide state.[26] Data were then collected at the National Synchrotron Light Source (Brookhaven National Laboratories, Upton, NY) on beamlines X9b and X3b (ring operating conditions: 2.8 GeV, 200−305 mA). A focused Si(111) double monochromator was used for energy selection along with a low-angle (4.5 mrad) Ni mirror for harmonic rejection. Energy calibrations were performed by recording a reference spectrum of Cu foil (first inflection point assigned to 8980.3 eV) simultaneously with the samples. All samples were maintained at 20 K throughout the data collection using a helium Displex cryostat. The spectra are reported as fluorescence data, which were recorded utilizing a 13-element Ge solid-state fluorescence detector (Canberra). Total count rates were maintained under 20 kHz per channel, and a deadtime correction of 3 μs was utilized (this had a negligible influence on the data). For XANES spectra, the primary hutch aperture height was set to 0.4 mm to obtain the maximum resolution (theoretical maximum is ~0.9 eV), while the hutch aperture was set to 1 × 2 mm, and data were obtained in 10 eV steps in the pre-edge region (8779−8958 eV), 0.3 eV steps in the edge region (8959−9023 eV), and 2.0 eV steps in the near-edge region. For EXAFS spectra, the primary hutch aperture was set to 0.8 mm, the hutch aperture was set to 1 × 8 mm, and data were obtained in 5.0 eV steps in the pre-edge region (8779−8958 eV), 0.5 eV steps in the edge region (8959−9023 eV), 2.0 eV steps in the near-edge region (9024−9278 eV), and 5.0 eV steps in the far-edge region (9279 eV−14.0 k). The EXAFS spectra represent the averaged sum of 20 spectra, while the XANES spectra represent the averaged sum of 3 spectra. After every other scan, the beam was moved to a different position on the sample to avoid potential radiation damage. All spectra were individually inspected prior to data averaging to ensure that sample decomposition in the beam was not occurring.

Chart 1

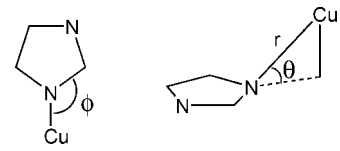

Data analysis was performed as previously described using the XAS analysis package EXAFS123.[27,28] The only deviation is that the numbers of scatterers in the individual shells were initially left as free parameters and then restrained to the nearest whole number. Single scatterer functions for Cu−N, Cu−O, and Cu−C interactions were constructed as previously described.[27,29] Multiple scattering (MS) pathways for the Cu−Im moiety were constructed by removal of the Cu−N single scattering interaction from 48 simulated reference spectra. These reference spectra were then used to construct the MS pathways in an analogous manner as before, where three refinable parameters are considered: the Cu−"N" distance (r(Im)), the in-plane angle (ϕ), and the out-of-plane angle (θ) (see Chart 1). For utilization of these MS pathways in the EXAFS analysis, we restrained r(Im) to be equal to the single scatterer Cu−N distance and then allowed the two angles to refine freely. Although data were collected to 14 k, data refinements were only performed out to $k = 12.0$ Å^{-1} due to noise at higher values of k. Best fits to the experimental data were determined by selecting the model that gave both chemically reasonable refinement parameters and the lowest value for the goodness-of-fit (GOF) parameter:

$$\mathrm{GOF} = \mathrm{ave}[(\chi - \chi_{\mathrm{sim}})/\mathrm{esd}_{\mathrm{data}}](n_{\mathrm{i}}/(n_{\mathrm{i}} - n_{\mathrm{p}}))^{1/2} \quad (1)$$

where n_{i} is the number of independent data points and n_{p} is the number of parameters used in the data simulations.

The bond valence sum (BVS) analysis[30] on all refined EXAFS models was applied according to

$$s_i = \exp[(r_{\mathrm{o}} - r)/0.37] \quad (2)$$

$$\mathrm{BVS} = \sum s_i \quad (3)$$

where r is the experimentally derived (EXAFS) bond length for ligand i and r_{o} is the reference bond length. The values used for r_{o} include $r_{\mathrm{Cu(II)N}} = 1.751$ Å, $r_{\mathrm{Cu(II)O}} = 1.679$ Å, and $r_{\mathrm{Cu(I)N}} = 1.595$ Å.

Results and Discussion

Aβ16Cu^{II} Cu K-Edge XAS. The Cu K-edge XAS obtained for the Cu^{II} adduct of Aβ16 is depicted in Figure 1. The edge region is characterized by a weak transition at 8979.7(1) eV that corresponds to the parity-forbidden Cu(1s→3d) transition

(26) Hou, L.; Shao, H.; Zhang, Y.; Li, H.; Menon, N. K.; Neuhaus, E. B.; Brewer, J. M.; Byeon, I. J.; Ray, D. G.; Vitek, M. P.; Iwashita, T.; Makula, R. A.; Przybyla, A. B.; Zagorski, M. G. *J. Am. Chem. Soc.* **2004**, *126*, 1992.

(27) Shearer, J.; Soh, P. *Inorg. Chem.* **2007**, *46*, 710.

(28) Scarrow, R. C. *EXAFS123*; Haverford College: Haverford, PA, 2005; www.Haverford.edu/chem./Scarrow/EXAFS123.

(29) Scarrow, R. C.; Strickler, B. S.; Ellison, J. J.; Shoner, S. C.; Kovacs, J. A.; Cummings, J. G.; Nelson, M. J. *J. Am. Chem. Soc.* **1998**, *120*, 9237. Scarrow, R. C.; Brennan, B. A.; Cummings, J. G.; Jin, H.; Duong, D. J.; Kindt, J. T.; Nelson, M. J. *Biochemistry* **1996**, *35*, 1078.

(30) Brown, I. D.; Altermatt, D. *Acta Crystallogr., Sect B* **1985**, *41*, 244. Thorp, H. H. *Inorg. Chem.* **1992**, *31*, 1585.

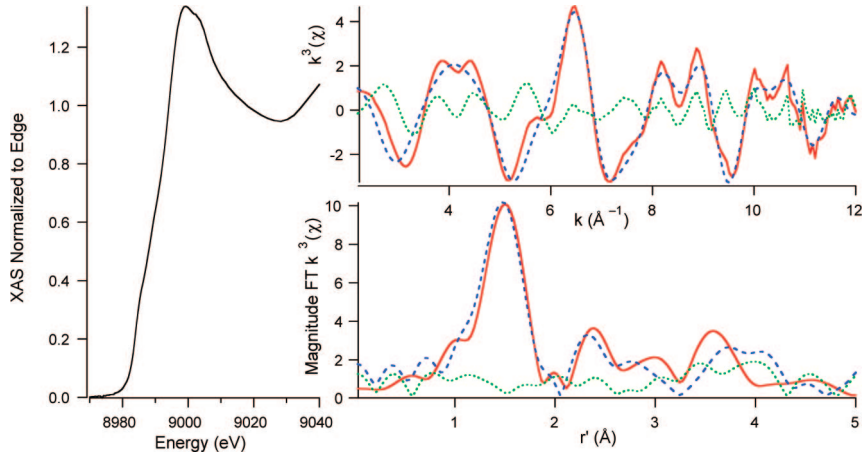

Figure 1. Cu K-edge XAS of Aβ16Cu^{II}. The left portion of the figure depicts the XANES region of the XAS. The right spectra depict the magnitude FT $k^3(\chi)$ (top) and $k^3(\chi)$ (bottom). The experimental data are the red spectra, the simulations to the data are the dashed blue spectra, and the difference between the experimental and simulations are the dotted green spectra.

Table 1. Parameters Used for Refinements to the Cu K-Edge X-ray Absorption Data for Aβ16Cu^{II} and Aβ16Cu^{I}

	Aβ16Cu^{II}	Aβ16Cu^{I}
pre-edge peak 1 (eV)	8979.3(7)	8984.1(2)
pre-edge peak 2 (eV)	8984.0(6)	–
E_o (eV)[a]	8988.7	8982.2
N/O Shell		
n[b]	3	2
r (Å)	1.938(12)	1.877(2)
σ^2 (Å^2)	0.0030(17)	0.0038(1)
N/O Shell		
n	1	–
r (Å)	2.07(2)	–
σ^2 (Å^2)	0.001(1)	–
Im Shell		
n	2	2
r (Å)[c]	1.938	1.877
σ^2 (Å^2)	0.003(2)	0.0057(1)
θ (deg)	8(3)	2(2)
ϕ (deg)	129(8)	130(11)
GOF	0.54	0.22
BVS	2.05	0.94

[a] For both refinements E_o was initially refined for the N-shell and then restrained. [b] Because of the way in which the MS pathways for the Im-shell were constructed, the first N/O shell contains the SS pathway for the Im shell. Therefore, the number of nonimidazole N/O scatterers is equal to the number of N/O scatterers in the first N/O shell minus the number of imidazole scatterers. [c] The distance of the imidazole shell was restrained to the distance of the first N/O scatterer.

and a shoulder in the edge region at 8986.8(1) eV that corresponds to a Cu(1s→4p + shakedown) transition.[31,32] The corresponding normal Cu(1s→4p) transition is not resolvable from the edge.

The EXAFS region was best modeled with Cu^{II} contained in a square-planar coordination environment with N/O ligation (Table 1, Figure 1). These refinements yielded three N/O scatterers at 1.938(12) Å and a fourth N/O scatterer at 2.07(2) Å. As can be seen, the magnitude Fourier transformed (FT) EXAFS shows strong outer-sphere scattering between r = 2 and 4 Å, which is characteristic of multiple scattering (MS) interactions between the Cu center and rigid ligands (i.e., imidazole rings from histidine residues). Using a MS analysis, we were able to determine that two of the three shorter N/O scatterers are imidazole scatterers. In addition to the distance parameter, the phase and amplitude functions utilized to refine the MS pathways also yielded the in-plane (ϕ) and out-of-plane (θ) Cu−His angles (see Chart 1). The resulting angles are best refined to $\theta = 8(3)°$ and $\phi = 129(8)°$. These are both consistent and reasonable for Cu−His ligation. We note that this represents the average of the two imidazole scatterers, and an analysis where the two imidazole scatterers were separated into different shells gave identical results. Addition of more or fewer imidazole functions to these refinements yielded either poorer fits to the data, unrealistic angles for the Cu−Im moiety, or instability in the data refinements. Attempts were made to identify a fifth longer ligand without success.

A BVS analysis was utilized to determine if these refinements make chemical sense.[30] In this empirical analysis the metal−ligand bond length derived from the EXAFS data is compared to a reference bond length, and a bond valence (s_i) is obtained. Summing up the bond valences for all of the metal−ligand distances in the complex gives the BVS. The strength of the BVS analysis is that it yields the same value for all transition metal complexes of the same metal type and oxidation state (e.g., Cu^{II}) *irrespective of coordination number and ligand type*. In the most widely applied variant of the BVS analysis, the reference bond lengths are chosen such that the resulting BVS will equal the transition metal ion's oxidation state. Therefore, for Cu^{II} the BVS should ideally be equal to 2. A BVS analysis is extremely helpful in evaluating EXAFS data, where the number of scatterers is the least reliable parameter obtained, because models that differ only by the number of scatterers in the same shells can be readily compared and contrasted on the basis of the BVS to determine which is most likely.

When a BVS analysis is applied to the above EXAFS data (Cu^{II} ligated by two *N*-imidazole scatterers and two N or O ligands), we calculate a BVS of 2.05 for a Cu^{II}(N^{Im})$_2$(O)$_2$ coordination model, either 2.13 or 2.16 for a Cu^{II}(N^{Im})$_2$(N)(O) coordination model (depending on the long vs short ligand identity), and 2.23 for the Cu^{II}(N^{Im})$_2$(N)$_2$ coordination model. The three possible models above with both N and O ligands in the primary coordination sphere give BVS values that are most

(31) Kau, L.-S.; Spira-Solomon, D. J.; Penner-Hahn, J. E.; Hodgson, K. O.; Solomon, E. I. *J. Am. Chem. Soc.* **1987**, *109*, 6433.
(32) DuBois, J. L.; Mukherjee, P.; Stack, T. D. P.; Hedman, B.; Solomon, E. I.; Hodgson, K. O. *J. Am. Chem. Soc.* **2000**, *122*, 5775.

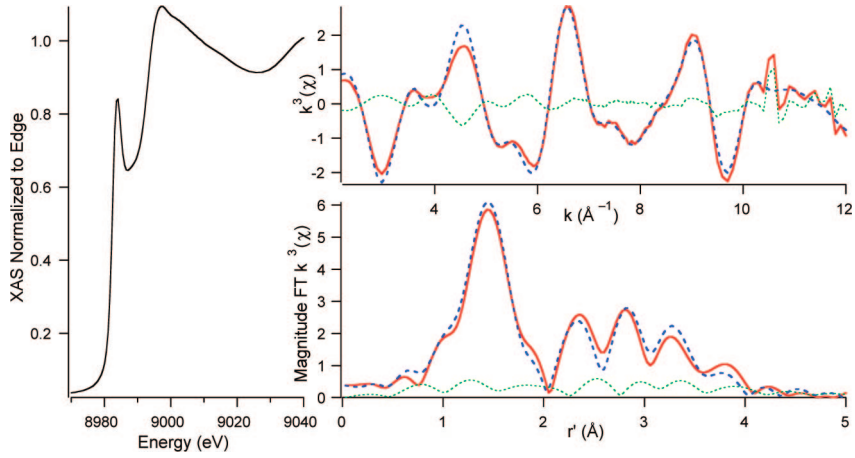

Figure 2. Cu K-edge XAS of Aβ16Cu^{I}. The left portion of the figure depicts the XANES region of the XAS. The right spectra depict the magnitude FT $k^3(\chi)$ (top) and $k^3(\chi)$ (bottom). The experimental data are the red spectra, the simulations to the data are the dashed blue spectra, and the difference between the experimental and simulations are the dotted green spectra.

consistent with Cu^{II}, while the coordination model with four nitrogen-based ligands gives a BVS that is likely too large to be consistent with Cu^{II}. Increasing the coordination number to five causes the resulting BVS to range between 2.40 and 2.84, depending on the number of N or O ligands, which are far too high to be consistent with Cu^{II}. Therefore, our XAS data are fully consistent with a four-coordinate Cu^{II} center ligated by two *N*-imidazole scatterers and two N or O ligands.

On the basis of these data alone, it is impossible to identify if the two non-imidazole ligands are nitrogen or oxygen donors. It is also impossible to determine the identity of the ligands. There is good evidence, however, that one of these ligands is an N-atom donor derived from the N-terminal amine nitrogen.[8,9,18] One consideration is whether the N-terminal amine group coordinates inter- or intramolecularly. In an intermolecular coordination mode, a Cu^{II} ion could be anchored to histidine residues in one peptide and bind the amino terminus from a second peptide. If each peptide binds one Cu^{II} ion and provides a ligand to another Cu^{II} ion via the amino terminus, a 1:1 Cu:peptide stoichiometry would result, but the molecular mass of the species would be twice that of a simple intramolecular AβCu complex. We performed gel filtration chromatography of Aβ16Cu^{II} to rule out this possibility (Figure S2) and found that the molecular weight of the Aβ16Cu^{II} species corresponds to a monomeric complex. In addition, the mass spectrometry results reported by Jiang et al. show that only a 1:1 complex is detected for Aβ40Cu^{II}.[10] Although neither of these results rules out a small population ($<\sim$1%) of dimer resulting from intermolecular copper ligation, the vast majority is due exclusively to intramolecular copper ligation.

We speculate that the other N/O-atom donor is likely an O-atom of a carbonyl group, perhaps from a carbonyl group of the peptide backbone. We suggest this possibility because one of our Cu^{II}−N/O-atom distances determined from the EXAFS refinements (2.07 Å) is close to the Cu^{II}−O-atom carbonyl distances measured in crystallographically characterized Cu^{II}−peptide complexes. Cu^{II} bound to a prion octarepeat peptide fragment has a Cu^{II}−O distance of 2.067 Å.[33] In that structure, Cu^{II} is coordinated to two backbone amides, one histidine, and a backbone carbonyl in the equatorial plane.[33] In addition, a 2.04 Å distance was reported for Cu^{II} coordinated to a carbonyl O-atom in the equatorial plane in a cylic bis-histidine peptide.[34] It should be noted that tyrosine has been ruled out as the O-atom donor ligand to Cu^{II} by numerous spectroscopic experiments.[9,11,14,18]

Our model for Aβ16Cu^{II} can be contrasted with a recently published model for Aβ40Cu^{II} by Morante and co-workers based on Cu K-edge XAS data.[35] Because the Cu^{II} coordinating residues are all found within the first 16 residues of the N-terminus of Aβ, Aβ16 is a good model of Cu^{II} coordination to Aβ40.[8,9,36] In the previous EXAFS study, the Cu^{II} ion was modeled in a five-coordinate square pyramidal geometry ligated by two His scatterers at 1.94 Å, one shorter His scatterer at 1.85 Å, a Tyr oxygen scatterer at 2.00 Å, and a water at 1.91 Å. In our view, the data presented by Morante are of insufficient quality to reliably separate similar scatterers at those distances; because the quality of the data presented by Morante is sufficient for analysis only between $k = 3.5$ and 10.5, the spectral resolution of their EXAFS data is only $\Delta r > 0.22$ Å at best (calculated from $\Delta r = \pi/(2\Delta k)$, given the quality of the data. Even with a sophisticated MS analysis, the reliable separation of the two different imidazole shells and the phenol shell would be extremely difficult (if not impossible) and would likely yield statistically meaningless structural parameters.

To discount changes in the microenvironment about the Cu center induced by the differences in the length of the Aβ fragment in this vs Morante's study, a reanalysis of the EXAFS data as presented in the paper by Stellato et al.[35] was undertaken. This reanalysis yields structural parameters consistent with our refinements from above (Table S2 and Figure S3). In fact, we find that because of the "penalty" imposed by the inclusion of additional refinement parameters in our error analysis, our four-coordinate (two imidazole/two N or O scatterers) model actually affords a slight statistical improvement over their five-coordinate model using Morante's data.

(33) Burns, C. S.; Aronoff-Spencer, E.; Dunham, C. M.; Lario, P.; Avdievich, N. I.; Antholine, W. E.; Olmstead, M. M.; Vrielink, A.; Gerfen, G. J.; Peisach, J.; Scott, W. G.; Millhauser, G. L. *Biochemistry* **2002**, *41*, 3991.

(34) Kojima, Y.; Hirotsu, K.; Matsumoto, K. *Bull. Chem. Soc. Jpn.* **1977**, *50*, 3222.

(35) Stellato, F.; Menestrina, G.; Serra, M. D.; Potrich, C.; Tomazzolli, R.; Meyer-Klaucke, W.; Morante, S. *Eur. Biophys. J.* **2006**, 340.

(36) Curtain, C. C.; Ali, F.; Volitakis, I.; Cherny, R. A.; Norton, R. S.; Beyreuther, K.; Barrow, C. J.; Masters, C. L.; Bush, A. I.; Barnham, K. J. *J. Biol. Chem.* **2001**, *276*, 20466.

Our reanalysis of the EXAFS data of Stellato et al. in-and-of itself obviously does not preclude a five-coordinate model, but a BVS analysis of the structural models does. Using their original refinement[35] (and our five-coordinate rerefinement of their data), we arrive at a BVS between 2.87 and 2.92, while four-coordinate refinements of these data yield a BVS that ranges between 2.02 and 2.31, depending on the CuN_2O_2 or CuN_4 models. This result means that a five-coordinate formulation for Aβ16Cu^{II} or Aβ40Cu^{II} is most likely incorrect. The issues with the original refinement of the low-resolution data collected by Stellato et al.,[35] our re-refinement of their data indicating that a five-coordinate geometry is untenable, and refinement of our own higher resolution data make us strongly favor a four-coordinate Cu^{II} model with two imidazole scatterers over a five-coordinate model for the Aβ−Cu^{II} adduct.

A very recent combined DFT/Cu K-edge XAS study by Streltsov et al.[15] on AβCu^{II} and several AβCu^{II} derivatives was performed at a resolution similar to that of our study (in fact, our data are virtually superimposable). That study arrived at a different Cu coordination environment than either Stellato or us; Streltsov et al. propose a six-coordinate structure with Cu^{II} ligation provided by three His imidazole nitrogens, both carboxylate oxygens from either Glu11 or Asp1, and another oxygen from a water molecule. Although the fit to the EXAFS data appears to be statistically valid, there are two reasons why the chemical interpretation of Streltsov et al. is questionable. There is general agreement from other spectroscopic data and recent theoretical work that Cu^{II} binds in a four-coordinate square planar coordination environment within Aβ.[8,9,18,19] Several of the spectroscopic methods applied to the AβCu^{II} complex cannot directly detect axial ligands, which means that a five- or six-coordinate Cu^{II} coordination geometry cannot be definitively ruled out, but the BVS produced by the Streltsov model is 2.64, which is considerably too high for Cu^{II}. Our BVS analysis is therefore key to affirming the general consensus from other spectroscopic and theoretical work that Cu^{II} is bound to Aβ in a four-coordinate geometry.

Aβ16Cu^{I} Cu K-Edge XAS. The Cu K-edge XAS of ascorbate-reduced Aβ16Cu^{I} is presented in Figure 2; similar data were obtained for Aβ40Cu^{I} (Figure S4), indicating identical coordination modes for Aβ40Cu^{I} and Aβ16Cu^{I}. A comparison of the edge regions of Aβ16Cu^{II} (Figure 1) vs Aβ16Cu^{I} shows that, upon reduction, the edge energy decreases by 4.2(6) eV, which is consistent with the reduction of Cu^{II} to Cu^{I}. Consistent with our results, Streltsov et al. report a >5 eV shift in edge energy upon reduction of Aβ16Cu^{II} with ascorbate.[15] The XANES region of the XAS for Aβ16Cu^{I} displays an intense pre-edge feature at 8984.1(2) eV, which is assigned as the Cu(1s→4p) transition.[31] For Cu^{I}, this feature is highly dependent on coordination geometry about the Cu^{I} center. The position and intensity of the Cu(1s→4p) transition observed for Aβ(16)Cu^{I} are consistent with either a two-coordinate linear geometry about Cu^{I} or possibly a three coordinate T-shaped geometry.[31,37] However, as will be shown, the reactivity of AβCu^{I} is most consistent with a two-coordinate linear geometry.

A best fit to the EXAFS yielded a two-coordinate geometry with two imidazole ligands coordinated to Cu^{I} at 1.877(2) Å (θ = 2(2)°, ϕ = 130(11)°; Scheme 1). Refinement of the data splitting the two imidazole scatters into different shells resulted in similar bond angles for the imidazole ligands (Figure S5).

Scheme 1

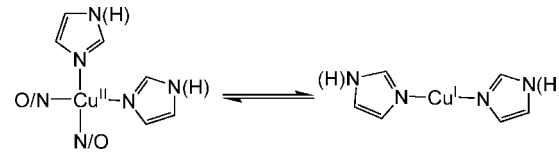

Attempts were made to solve for a three-coordinate ligation environment for Aβ16Cu^{I}.[16] In all cases, a T-shaped geometry could not be refined: the shell containing a third imidazole scatterer was always placed at a distance nearly identical to the shell containing the other two imidazole scatterers. A BVS analysis of the two refinements yields BVS = 0.94 for the two-coordinate complex and 1.42 for the three-coordinate complex. We therefore favor a linear two-coordinate Cu^{I} coordination environment for Aβ16Cu^{I} on the basis of the Cu K-edge XAS coupled with the BVS analysis.

AβCu^{II}/AβCu^{I} EPR Spectroscopy. Spectra for both Aβ16Cu^{II} and Aβ40Cu^{II} samples before and after the addition of ascorbate are shown in Figure 3. After the addition of ascorbate, the EPR signal decreases due to the disappearance of the AβCu^{II} complex, indicating the formation of the d^{10}, EPR-silent AβCu^{I} complex. Maiti et al. reported that the reduction of Aβ16Cu^{II} and O_2-reoxidation of Aβ16Cu^{I} are completely reversible, as observed by fluorescence spectroscopy.[14] This observation is inconsistent with our EPR spectroscopic data.

For the Aβ16Cu^{II} sample, spectral integration indicates that approximately 90% of the initial AβCu^{II} content is recovered in a sample treated with 1.2 equiv of ascorbate under inert atmosphere followed by 19 h of air exposure. We note that, if an ascorbate-treated sample is immediately treated with excess Ir(IV), the initial AβCu^{II} signal hyperfine intensity recovers entirely (Figure S6). In this case, spectral integration to quantify the AβCu^{II} concentration is not reliable because of the contribution from the broad EPR signal of unreacted Ir^{IV}. For Aβ40Cu^{II}, a similar pattern of sluggish O_2 reactivity was observed even under conditions where only 0.5 equiv of ascorbate was added (Figure 3B). The Cu^{II} concentrations for the 13 and 28 min time points for the AβCu^{II} + ascorbate reaction are the same within error (Figure 3B, inset), which indicates that the reduction reaction is complete after this time. After 19 h in air, the Cu^{II} concentration recovers to approximately 80% of its initial value. A matched sample treated with a 2-fold excess of ascorbate recovered only 60% of the initial Cu^{II} signal after 3 d in air (Figure S7). Finally, Aβ40Cu^{II} was reduced with a 4-fold excess of ascorbate in air-saturated solution (Figure S8). The EPR signal from Aβ40Cu^{II} decreased to about 15% of the initial signal. Like the sample treated with excess ascorbate under Ar, only about 60% of the initial Cu^{II} intensity is recovered in this sample after extended incubation (5 d) at room temperature.

In all of the samples prepared anaerobically and then exposed to oxygen, the Cu^{II} spectral shapes are the same before and after ascorbate addition, suggesting that Cu^{II} is bound in its original coordination site after its reduction and reoxidation. The experiment performed in air, however, has slight differences in the spectral shapes before and after ascorbate addition (Figure S8, inset). In that case, the post-ascorbate addition spectrum appears to contain contributions from two different Cu^{II} species. The appearance of a new Cu^{II} signal could be due to protein modification from carbonate radicals that are generated upon

(37) Himes, R. A.; Park, G. Y.; Barry, A. N.; Blackburn, N. J.; Karlin, K. D. *J. Am. Chem. Soc.* **2007**, *129*, 5352.

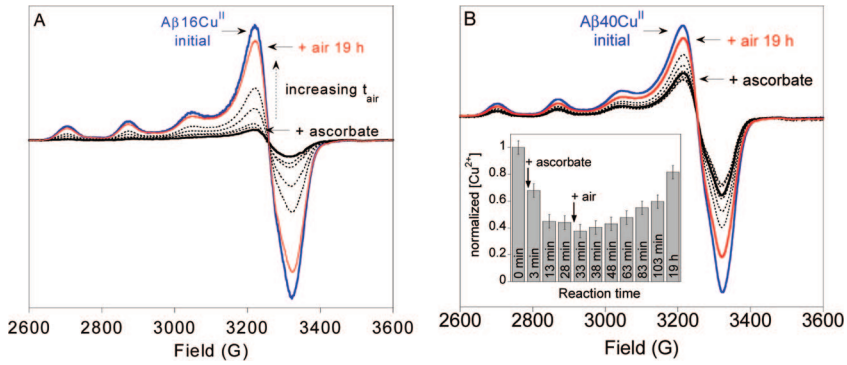

Figure 3. 20 K EPR spectra of the reduction of AβCu^{II} by ascorbate and subsequent reoxidation in air: (A) 250 μM Aβ16Cu^{II} (blue) + 1.2 equiv of ascorbate (solid black line) followed by addition of air (dotted lines, red line); (B) 100 μM Aβ40Cu^{II} (blue) + approximately 0.5 equiv of ascorbate (solid black line) followed by addition of air (dotted lines, red line). The inset to panel B shows the normalized Aβ40Cu^{II} signal area as a function of total reaction time. EPR conditions are given in the Materials and Methods section.

redox cycling of Cu.[38,39] Samples made in air-saturated buffer contain more CO_2 than degassed samples. Addition of carbonate radicals to proteins does not fragment the protein,[39] but instead introduces modifications. Such modifications might change the protein structure and/or metal binding sites, leading to our observation of two types of Cu^{II} EPR signals in aerobic samples treated with ascorbate.

The fluorescence data of Miati et al. indicate that the Aβ16Cu^{II} complex is completely regenerated upon exposure of the AβCu^{I} complex to O_2.[14] In contrast, our EPR spectroscopic results indicate that the initial full concentration of AβCu^{II} complex is not regenerated upon oxidation of AβCu^{I}. As EPR spectroscopy is a direct indicator of the Cu^{II} coordination environment, whereas tyrosine fluorescence quenching is an indirect measure of A$\beta-$Cu^{II} coordination, our more sensitive data strongly suggest the loss of Cu^{II} binding affinity toward Aβ.

There are several possible explanations for why an EPR signal from AβCu^{II} does not reappear entirely upon air exposure of anaerobic samples treated with ascorbate. One possibility is that some fraction of Cu^{II} is released from the peptide because of oxidative decomposition of the peptide. This released Cu^{II} will bind to phosphate buffer to make an antiferromagnetically coupled Cu^{II} polymer that is EPR silent. Our HPLC results (*vide infra*) are consistent with oxidative damage of the peptide. Another possibility is that a stable Cu^{I} compound or some other type of copper cluster forms that is EPR silent.

The reaction of AβCu^{II} with a large excess of reductant has been reported to produce hydrogen peroxide, hydroxyl radicals, and tyrosine radicals.[3,13,40−42] Tyrosyl radical, in particular, has been proposed as an intermediate in ROS generation by the AβCu complex.[40,42,43] Under our conditions, AβCu^{II} with ascorbate does not produce a detectable amount of tyrosine radical, a species that is easily identifiable by low-temperature EPR spectroscopy.[44] This result indicates that this radical does not reach a steady-state concentration above our detection limit. Barnham et al. proposed catalytic tyrosine radical formation as part of the ROS-generating mechanism for AβCu,[42] which contradicts peptide oxidation detected by mass spectrometry, showing that histidine oxidation appears prior to tyrosine oxidation and cross-linking reactions.[45,46] Thus, it remains unclear whether tyrosine radical formation precedes, is concerted with, or follows hydrogen peroxide/hydroxyl radical production.

Assessment of Oxidative Damage of Aβ16 following Multiple Cu Redox Cycles. Our EPR results clearly show that regeneration of AβCu^{II} is not quantitative following redox cycling, which may be indicative of peptide damage to the copper-ligating residues of Aβ or other processes that change the physiochemical nature of Aβ16, as has previously been observed.[47] We probed the supposition that peptide damage may be responsible for the nonquantitative regeneration of AβCu^{II} by following multiple redox cycles using HPLC (Figure 4). Prior to reduction of Aβ16Cu^{II} by ascorbate, the metallopeptide shows one distinct peak in the chromatogram. Following reduction of Aβ16Cu^{II} with 1 equiv of ascorbate and 19 h of air oxidation, three new peaks have appeared in the chromatogram, and the amount of Aβ16Cu^{II} has decreased by 33% of its original concentration compared to a peptide standard. After a second redox cycling under identical conditions, more Aβ16Cu^{II} has been lost (56% of its original concentration), the additional peaks have increased in intensity, a fourth peak has grown in, and there is a significant amount of material that comes off the column only toward the end of the HPLC run (and in the column wash), which is indicative of peptide oligomerization. After a third and final redox cycling, the amount of Aβ16Cu^{II} remaining in solution is 39% of its original concentration, while the amount of material coming off at the end of the run has increased significantly, indicating increased peptide aggregate formation, and a fifth broad peak between 11 and 13 min has appeared in the chromatogram.

The HPLC redox cycling results confirm the EPR results from above: damage to Aβ16Cu^{II} is occurring following multiple redox cycles. Control HPLC and GPC studies demonstrate that Aβ16Cu^{II} does not undergo significant damage or oligimerization if a reductant is not added to solution (Figures S2 and S9). This strongly suggests that redox cycling is accelerating the deterioration of monomeric Aβ16Cu^{II}. It is likely that oxidative damage to Aβ16 is occurring here similar to that previously reported by Schöneich and Williams, who observed predominant oxidation of His13 and His14.[47] We are currently in the process of identifying the Aβ modification sites and the oxidized products to confirm this supposition.

These HPLC results indicate that slightly more oxidative damage to Aβ16Cu^{II} is occurring during redox cycling than indicated by EPR, as there is a significantly larger decrease in soluble monomeric Aβ16Cu^{II} observed by HPLC than EPR. There are at least three possible explanations for this observation.

(38) Ramirez, D. C.; Mejiba, S. E.; Mason, R. P. *J. Biol. Chem.* **2005**, *280*, 27402.
(39) Ramirez, D. C.; Gomez-Mejiba, S. E.; Corbett, J. T.; Deterding, L. J.; Tomer, K. B.; Mason, R. P. *Biochem. J.*, published online as Immediate Publication Sept 2, 2008 (http://dx.doi.org/10.1042/BJ20070722).

The first is that one (or more) of the modified Aβ16 products is capable of coordinating Cu^{II} in a ligand environment nearly identical to that of unmodified Aβ16. Another explanation is that redox cycling produces soluble, cross-linked $A\beta16Cu^{II}$ oligomers, which are spectroscopically similar by EPR but distinguishable by HPLC. The third explanation is that the EPR samples contained less oxygen than the HPLC samples. The buffer was the same for both sets of samples, so the O_2 solubility in the solvent system is the same. However, following air exposure, EPR samples were sealed and not reopened, which means that no additional air (and, therefore, O_2) was introduced. We calculate that there is 14.7 μmol of O_2 in the headspace of the EPR tube compared to 0.01 μmol of Cu in the sample, which represents a 1500-fold excess of O_2 over Cu. Nevertheless, the HPLC samples were prepared and handled in air, so the amount of air in the samples could be higher than in the EPR samples.

Summary and Biological Implications

In this study we have shown that $A\beta Cu^{II}$ can readily undergo reduction by the biologically relevant reductant ascorbate.[48] By XAS we have shown that, upon reduction of $A\beta16Cu^{II}$ and $A\beta40Cu^{II}$ with ascorbate, linear His_2-Cu^{I} adducts are formed (Scheme 1). Our XAS analysis is consistent with the observed O_2 reactivity displayed by $A\beta16Cu^{I}$ and $A\beta40Cu^{I}$. Following reduction of $A\beta Cu^{II}$ with stoichiometric amounts of ascorbate, solutions of $A\beta16Cu^{I}$ or $A\beta40Cu^{I}$ are not highly sensitive to O_2, similar to solutions of two coordinate Cu^{I} model complexes.[37,49] Similarly, solutions of two-coordinate Cu^{I} complexes are not susceptible to oxidation by dioxygen.[37,49] In contrast, three-coordinate Cu^{I} centers are highly reactive toward dioxygen, typically undergoing oxidation to Cu^{II} instantaneously upon exposure to dioxygen.[37,50] Therefore, the dioxygen reactivity of $A\beta16Cu^{I}$ is consistent with our XAS analysis.

A recent study by Karlin and co-workers is also consistent with our formulation of a linear diimidazole$-Cu^{I}$ ligation scheme for $A\beta16Cu^{I}$.[37] In that study, a series of His−His dipeptides coordinated to Cu^{I} formed linear two-coordinate copper centers with Cu−imidazole bond lengths ranging from 1.863 to 1.876 Å. These two-coordinate Cu^{I} dipeptides were not prone to oxidation by O_2. However, upon the addition of a third imidazole-based ligand to the Cu^{I} dipeptides, rapid oxidation of Cu^{I} to Cu^{II} was noted in that study. Again, the O_2 reactivity of both $A\beta16Cu^{I}$ and $A\beta40Cu^{II}$ is most consistent with a linear diimidazole$-Cu^{I}$ ligation scheme.

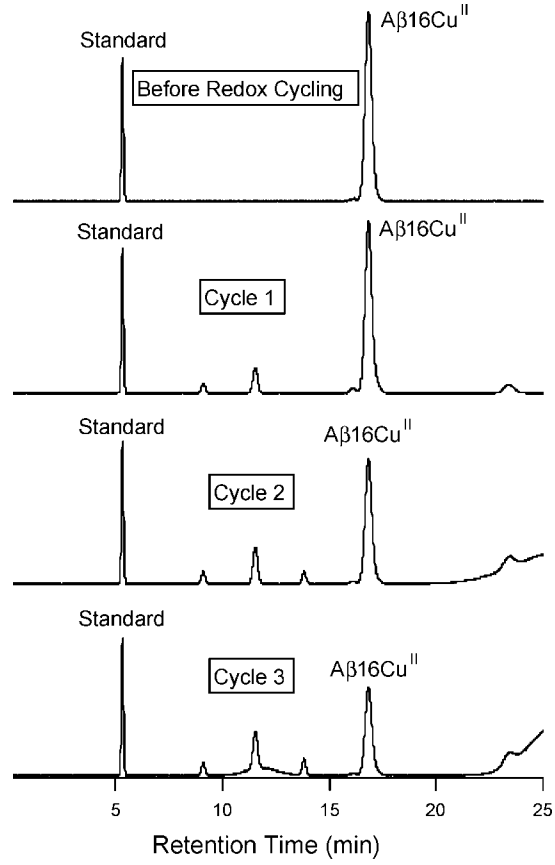

Figure 4. HPLC chromatograms of $A\beta16Cu^{II}$ following multiple redox cycling using ascorbate in air.

In addition to providing experimental precedence in support of our coordination mode for $A\beta16Cu^{I}$ and $A\beta40Cu^{I}$, Karlin's study hints at the identity of the two His residues ligated to Cu^{I} in these metallopeptides. The copper-binding domain of Aβ contains two adjacent His residues at positions 13 and 14, making it reasonable to speculate that His13 and His14 are the residues involved in Cu^{I} coordination in Aβ. Computational studies by both us and Karlin indicate that the linear Cu^{I} bis-His motif is not strained, and we in fact arrive at nearly identical structural parameters for the $[Cu^{I}(His)_2]^{+}$ metallopeptide using high-level double-hybrid DFT methods as we determined by EXAFS (Figure S10, Table S3). Indeed, mass spectrometry of oxidative damage products generated upon reduction of $A\beta Cu^{II}$ with ascorbate indicates that His13 and His14 are preferentially oxidized at short reaction times,[46] not His6, suggesting His13 and His14 provide the ligands to Cu^{I}. Although it is possible that one of these two histidines is damaged because of proximity to copper and not direct ligation, it is difficult to explain why His6 is not damaged if it is one of the two histidine ligands to copper.

Another finding of this study that has broad implications for our understanding of the etiology of the $A\beta Cu$ complex is the oxidative damage of the reduced metallopeptides following oxidation by O_2. It has been shown that $A\beta Cu^{II}$ in the presence of reductants generates ROS.[13,51] We ascribe incomplete recovery of the $A\beta Cu^{II}$ EPR signal to ROS-induced peptide

(40) Atwood, C. S.; Perry, G.; Zeng, H.; Kato, Y.; Jones, W. D.; Ling, K. Q.; Huang, X.; Moir, R. D.; Wang, D.; Sayre, L. M.; Smith, M. A.; Chen, S. G.; Bush, A. I. *Biochemistry* **2004**, *43*, 560.
(41) Haeffner, F.; Smith, D.; Barnham, K.; Bush, A. *J. Inorg. Biochem.* **2005**, *99*, 2403.
(42) Barnham, K. J.; Haeffner, F.; Ciccotosto, G. D.; Curtain, C. C.; Tew, D.; Mavros, C.; Beyreuther, K.; Carrington, D.; Masters, C. L.; Cherny, R. A.; Cappai, R.; Bush, A. I. *FASEB J.* **2004**, *18*, 1427.
(43) Tickler, A. K.; Smith, D. G.; Ciccotosto, G. D.; Tew, D. J.; Curtain, C. C.; Carrington, D.; Masters, C. L.; Bush, A. I.; Cherny, R. A.; Cappai, R.; Wade, J. D.; Barnham, K. J. *J. Biol. Chem.* **2005**, *280*, 13355.
(44) Szalai, V. A.; Brudvig, G. W. *Biochemistry* **1996**, *35*, 15080. Szalai, V. A.; Brudvig, G. W. *Biochemistry* **1996**, *35*, 1946. Szalai, V. A.; Kühne, H.; Lakshmi, K. V.; Brudvig, G. W. *Biochemistry* **1998**, *37*, 13594. Stubbe, J.; van der Donk, W. A. *Chem. Rev.* **1998**, *98*, 705.
(45) Schoneich, C. *Ann. N.Y. Acad. Sci.* **2004**, *1012*, 164.
(46) Pogocki, D.; Schoneich, C. *Chem. Res. Toxicol.* **2002**, *15*, 408.
(47) Schöneich, C.; Williams, T. D. *Chem. Res. Toxicol.* **2002**, *15*, 717.
(48) Rice, M. E. *Trends. Neurosci.* **2000**, *23*, 209.
(49) Sorrell, T. N.; Jameson, D. L. *J. Am. Chem. Soc.* **1983**, *105*, 6013. Sanyal, I.; Strange, R. W.; Blackburn, N. J.; Karlin, K. D. *J. Am. Chem. Soc.* **1991**, *113*, 4692. Sanyal, I.; Strange, R. W.; Blackburn, N. J.; Karlin, K. D. *J. Am. Chem. Soc.* **1993**, *115*, 11259.
(50) Lewis, E. A.; Tolman, W. B. *Chem. Rev.* **2004**, *104*, 1047.

damage, in particular histidine oxidation,[12,40,47,52] that precludes Cu^{II} binding in the native coordination site. Our HPLC results also indicate that multiple redox cycling produces significantly more Aβ damage following each cycle; there is a nonlinear increase in Aβ damage following each redox cycle. This leads us to predict that, when aerobic solutions of AβCu^{II} are redox-cycled via addition of excess ascorbate, an evolving and heterogeneous mixture of Cu species is created: copper ions bound to modified and unmodified peptide and copper ions not bound to the peptide are all present.

It has been shown that addition of an exogenous chelator to solutions of AβCu^{II} treated with ascorbate retards hydrogen peroxide production.[53] This result is entirely consistent with the fact that chelated Cu^{II} is reduced more slowly by ascorbate than "free" Cu^{II} ion.[54] Such heterogeneity of the Aβ/Cu^{II}/reductant reaction mixture and details of the rate constant/mechanism differences between bound and unbound copper have not been considered carefully previously. In our view, these critical issues call into question measurements of the rates of hydrogen peroxide and/or hydroxyl radical production by AβCu^{II}, which have assumed that a single species (Cu-ligated Aβ) is responsible for ROS formation.[10,13] Both Cu^{II} that is not bound to peptide and copper-ligated Aβ may be producing ROS, but we believe Cu^{II} released from oxidatively modified Aβ is the principal ROS generator in those experiments.

Together, these findings suggest several hypotheses concerning Aβ and its role in neurodegeneration. First, under redox-cycling conditions, oxidative damage to Aβ inhibits its ability to bind Cu, and thus will promote oxidative stress in neuronal tissue. Also, these data point toward the supposition that copper-induced ROS generation mediates Aβ aggregation, as has been previously suggested.[40,55] Upon multiple rounds of redox cycling of Aβ16Cu^{II}, it appears that significant Aβ16 aggregation occurs, perhaps via covalent cross-linking. Oxidative modification of Aβ increases its propensity to aggregate, which has been hypothesized to increase Aβ oligomer formation and/or plaque deposition in AD.[40,42,56]

Finally, we propose that AβCu may be neuroprotective[57] if it forms a Cu^{I} complex rather than a Cu^{II} complex *in vivo*. We come to the conclusion that AβCu might be neuroprotective on the basis of our EXAFS results, which are consistent with the O_2-stable linear Cu^{I} coordination geometry, and a thermodynamic square scheme (Scheme 2). This scheme predicts a higher affinity of Aβ for Cu^{I} than for Cu^{II} because the midpoint potential of AβCu^{II}/AβCu^{I} is higher (0.28 V[10] vs NHE) than that of free Cu^{II}/Cu^{I} (0.158 V vs NHE).[58] Note that the magnitude of the affinity of Aβ for Cu^{II} has no effect on the *relative* affinities of Aβ for Cu^{I} vs

Scheme 2

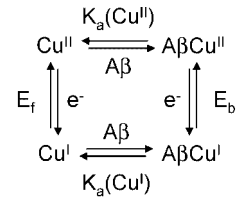

$$E_b - E_f = 0.059 \times \log\left(\frac{K_a(Cu^{I})}{K_a(Cu^{II})}\right)$$

Cu^{II}. Our assumption that the "free" Cu^{II}/Cu^{I} potential is lower than that of the AβCu^{II}/AβCu^{I} complex is supported by electrochemistry experiments that showed that Cu^{II} in buffer is reduced at a lower potential than AβCu^{II}/AβCu^{I} in the same buffer.[10] If Aβ has a higher affinity for Cu^{I} than Cu^{II} and the AβCu^{I} complex is sluggish to react with O_2, damage from Cu ions will be abrogated in the presence of Aβ compared to Cu^{II}/Cu^{I} that is not bound to peptide.

The redox-cycling of AβCu depends on the concentrations of ascorbate and O_2 *in vivo*. Extracellular fluid that surrounds mammalian neurons, and is in equilibrium with cerebral spinal fluid (CSF), contains 200−400 μM ascorbate.[48] The pO_2 of CSF has been measured to be 31−51 mmHg by invasive methods.[59] More recently, values obtained using fluid-attenuated inversion recovery (FLAIR) magnetic resonance imaging on humans are 54 ± 18 (lateral ventricles), 67 ± 1 (cisterna magna), 106 ± 42 (cortical sulci), and 130 ± 49 mmHg (third ventrical), which gives an average of about 90 mmHg in CSF.[60] For comparison, the pO_2 in the trachea is about 150 mmHg. Thus, the concentration of O_2 in CSF is about 2-fold lower than in air-saturated solutions at 37 °C. Although our experiments were performed at room temperature instead of 37 °C and, therefore, the rates are different from those at 37 °C, we find that the Aβ40Cu^{II} species can be reduced to Aβ40Cu^{I} in an environment containing substantially more O_2 (air-saturated buffer) than is present in CSF. Although speculative, our idea that AβCu^{I} is the dominant species *in vivo* is consistent with our findings and represents a neuroprotective mechanism for AβCu that has not been proposed previously.

Acknowledgment. This work was funded by Alzheimer's Association Grant IIRG-07-5821 (V.A.S.) and NIH grant no. P20 RR-016464 from the INBRE Program of the National Center for Research Resources (J.S.). Use of the National Synchrotron Light Source, Brookhaven National Laboratory, was supported by the U.S. Department of Energy, Office of Science, Office of Basic Energy Sciences, under Contract No. DE-AC02-98CH10886.

Note Added in Proof. After this manuscript was accepted for publication, another paper on XAS of AβCu^{I} appeared [Himes et al. *Angew. Chem. Int. Ed.* **2008**, *47*, 9084]. Two of the model Aβ peptides in that study also bind Cu^{I} in a linear bis-His coordination environment.

Supporting Information Available: XAS spectra of Aβ40Cu^{I}, additional refinements to the EXAFS region of

(51) Huang, X.; et al. *J. Biol. Chem.* **1999**, *274*, 37111.
(52) Lim, J.; Vachet, R. W. *Anal. Chem.* **2003**, *75*, 1164.
(53) Deraeve, C.; Pitie, M.; Meunier, B. *J. Inorg. Biochem.* **2006**, *100*, 2117.
(54) Taqui Khan, M. M.; Martell, A. E. *J. Am. Chem. Soc.* **1967**, *89*, 7104. Taqui Khan, M. M.; Martell, A. E. *J. Am. Chem. Soc.* **1967**, *89*, 4176.
(55) Smith, D. G.; Cappai, R.; Barnham, K. J. *Biochim. Biophys. Acta* **2007**, *1768*, 1976.
(56) Yoburn, J. C.; Tian, W.; Brower, J. O.; Nowick, J. S.; Glabe, C. G.; Van Vranken, D. L. *Chem. Res. Toxicol.* **2003**, *16*, 531. Smith, D. P.; Ciccotosto, G. D.; Tew, D. J.; Fodero-Tavoletti, M. T.; Johanssen, T.; Masters, C. L.; Barnham, K. J.; Cappai, R. *Biochemistry* **2007**, *46*, 2881.
(57) Zou, K.; Gong, J. S.; Yanagisawa, K.; Michikawa, M. *J. Neurosci.* **2002**, *22*, 4833.
(58) Weast, R. C., Ed. *Handbook of Chemistry & Physics*, 51st ed.; The Chemical Rubber Company: Cleveland, OH, 1970.
(59) Jarnum, S.; Lorenzen, I.; Skinhoj, E. *Neurology* **1964**, *14*, 703. Ganshirt, H. *Wien Med. Wochenschr.* **1966**, *116*, 953.
(60) Zaharchuk, G.; Martin, A. J.; Rosenthal, G.; Manley, G. T.; Dillon, W. P *Magn. Reson. Med.* **2005**, *54*, 113. Zaharchuk, G.; Busse, R. F.; Rosenthal, G.; Manley, G. T.; Dillon, W. P. *Proc. Int. Soc. Magn. Reson. Med.* **2005**, *13*, 66.

Aβ16Cu^{II} and Aβ16Cu^{I}, EPR spectra of the reoxidation of Aβ16Cu^{I} by Ir(IV), reduction/air reoxidation of Aβ40Cu^{II} with excess ascorbate in anaerobic solution and in air-saturated buffer, digitized XAS data from Stellato et al.,[35] our re-refinement of EXAFS data from Stellato et al.,[35] geometry-optimized structure for $(Cu^{I}(His)_2)^+$, control HPLC and GPC chromatograms of air-exposed AβCu^{II} (Figures S1−S11; Tables S1−S3), and complete ref 51. This material is available free of charge via the Internet at http://pubs.acs.org.

JA805940M